

Relationship between Sintering Conditions, Microstructure and Properties of Alumina 10 vol% Zirconia Nanocomposites

F. Kern*

Institut für Fertigungstechnologie keramischer Bauteile, Universität Stuttgart, (Institute for Manufacturing Technologies of Ceramic Components and Composites, University of Stuttgart), 70569 Stuttgart, Allmandring 7b, Germany

received September 21, 2011; received in revised form October 5, 2011; accepted October 12, 2011

Abstract

Zirconia-toughened alumina (ZTA) ceramics of various compositions have high relevance in the field of mechanical engineering for cutting tools and wear parts as well as in biomedical applications for hip and knee implants.

In this study a matrix of submicron size α -alumina is reinforced with 10 vol% unstabilized zirconia nanoparticles. The ZTA ceramics were consolidated by means of hot pressing at 1400–1550 °C at 60 MPa axial pressure for 1 h in order to test the influence of the sintering conditions on the mechanical properties, microstructure and phase composition. Despite the conventional mixing and milling method used, ZTA nanocomposites of high homogeneity were obtained. Low sintering temperatures result in ultra-fine-grained materials with high hardness. High strength of 900–1050 MPa was observed over the whole sintering temperature range, while toughness rises with sintering temperature. A clear correlation between transformability of the tetragonal phase and toughness cannot be identified. Highest strength was found for ZTA with a low initial monoclinic content and high transformability. Increasing sintering temperatures led to only slight microstructural coarsening but to a migration of zirconia particles and rising monoclinic content. Associated with these effects, a gradual shift from transformation toughening to microcrack toughening was observed.

Keywords: ZTA, nanocomposite, microstructure, phase composition

I. Introduction

ZTA materials were designed more than 30 years ago to combine the high hardness and abrasion resistance of alumina with an additional toughness increment derived from a zirconia dispersion. The predominant reinforcement mechanisms identified in ZTA are transformation toughening and microcracking¹. Reinforcement with large monoclinic zirconia grains leads to microcrack toughening with little or no strength increase². Transformation toughening, which provides both strength and toughness, is achieved by incorporating small tetragonal grains of approximately 0.5 μm into the alumina matrix³. The evolution of the microstructures is strongly dependent on the zirconia content. At low zirconia volume contents $V(\text{ZrO}_2) < 5 - 7.5\%$, the dispersion cannot block all four junctions between the alumina grains. Thus alumina grains may grow and incorporate zirconia leading to intra- or intra-inter type nanocomposites. At $V(\text{ZrO}_2) > 7.5\%$, ZTA with a stable predominantly inter-type microstructure is formed, which shows little matrix grain growth⁴. Intra- and intragranular zirconia exhibit different transformation characteristics⁵. The amount of stabilizer – preferentially yttria – which is required to keep the tetragonal zirconia dispersion stable against spontaneous

transformation upon cooling is dependent on the volume fraction, grain size and structural homogeneity.

While the percolation theory predicts an upper limit of ~ 16 %, under practical conditions only about 10 vol% zirconia can be added without stabilization⁶. Residual cooling stresses are caused by the CTE mismatch of alumina and zirconia leaving the alumina matrix under compressive and tetragonal zirconia under tensile stress. Zirconia thus becomes very transformable. In most cases a considerable amount of monoclinic is observed in the as-fired samples as the zirconia can escape the tensile stress by transformation, which is associated with volume increase. The extent of transformation is strongly dependent on processing, especially the milling and firing cycle. A stress-neutral state is achieved at a monoclinic content of ~20 %⁷. It was shown that by increasing the uniformity in the zirconia particle size and the homogeneity of distribution, the mechanical properties of ZTA can be improved. To date, the best results were obtained by coating alumina with zirconia nanoparticles obtained from zirconia precursors⁸. This, however, requires additional processing effort and increases the powder cost significantly. A scale-up to pilot plant size has yet not been demonstrated. In this study an attempt was therefore made to use a mixing and intensive milling approach and obtain highest

* Corresponding author: frank.kern@ifkb.uni-stuttgart.de

possible homogeneity based on selection of ultrafine and only weakly agglomerated zirconia powder.

II. Experimental

The starting powders chosen were α -alumina APA 0.5 (Ceralox, USA) with a particle size $d_{50} = 0.3 \mu\text{m}$ and $S_{\text{BET}} = 8 \text{ m}^2/\text{g}$ and monoclinic zirconia nanopowder UEP (Daiichi Kagaku Kigenso, Japan) with $S_{\text{BET}} = 23.6 \text{ m}^2/\text{g}$. These manufacturer's specifications were verified with laser granulometry using the Mie method (Malvern, Germany). The primary crystallite size of the zirconia was determined by means of Scherrer analysis⁹. 171 g α -alumina APA 0.5 and 29 g zirconia UEP were milled in 250 ml 2-propanol in a polyoxymethylene jar for 4 h at 600 rpm using 600 g 3Y-TZP milling balls. The resulting slurry was dried at 90 °C for 12 h. After being screened through a 100- μm mesh the powder was ready for further processing. Hot pressing (KCE, Germany) was performed in a rectangular (42.5 x 22.5 mm²) boron-nitride-clad graphite die. After evacuation and pre-loading with 2 MPa, the press was heated at 50 K/min to final temperature of 1400–1550 °C. The final temperature was varied in 25 K increments and kept for 1 h dwell at 60 MPa axial pressure. Two plates were sintered per hot pressing cycle. The plates were cooled in an argon atmosphere in the press with the heater switched off. The sintered samples were prepared for characterization by lapping with 15- μm diamond suspension and subsequent polishing with 15- and 3- μm diamond suspension for 45 min each (Struers, Denmark). The two polished plates from each pressing run were then cut into bars measuring 4 mm in width and ~2 mm in thickness on a diamond wheel (Struers, Denmark). To eliminate cutting grooves, the sides were machined to a 3- μm finish by lapping and polishing. Edges were beveled by grinding with a 40- μm diamond disk and polishing with 15- μm diamond suspension. Remaining pieces were kept for hardness testing and XRD analysis.

The bending strength of 10 bars of each parameter set was measured in a 3-pt setup with 15 mm outer span according to DIN EN 6872 (Hegewald & Peschke, Germany). Vickers hardness HV_{10} (5 indents each, Bareiss, Germany) and $HV_{0.1}$ (12 indents, Fischerscope, Germany) were measured. The indentation modulus was calculated from the unloading curve of the microhardness measurement. Fracture toughness K_{IC} was measured with two independent methods. Indentation toughness was measured by means of direct crack length measurement on five HV_{10} indents using the Anstis calculation model¹⁰. Indentation strength in bending (ISB) tests were performed on four samples pre-notched with a HV_{10} indent on the middle of the tensile side in a 3-pt setup with 15-mm span using Chantikul's calculation model¹¹.

Samples for microstructural analysis were thermally etched (1400 °C/30 min/air). Scanning electron microscopy was performed in secondary electron mode using a low acceleration voltage of 3 kV with conductive carbon coating (Zeiss, Germany). The phase composition of polished surfaces and of fracture faces was studied with XRD (Bruker, Germany, $\text{CuK}\alpha$, graphite monochromator). The intensities of the monoclinic (-111) and (111) reflexes and the tetragonal (101) reflex in the

2 θ –33° 2 θ -range were determined and the phase fractions were calculated using the calibration curve proposed by Toraya¹². Grain sizes were determined with the line intercept method¹³. Density was measured by means of immersion in water using Archimedes' principle.

III. Results and Discussion

(1) Characterization of starting powders

The grain size distributions of the starting powders measured by laser granulometry are shown in Fig. 1. Alumina APA0.5 shows a narrow and monomodal grain size distribution with $d_{50} = 420 \text{ nm}$ ($d_{10} = 210 \text{ nm}$, $d_{90} = 780 \text{ nm}$), which fits quite well with the manufacturer's specification. Zirconia UEP has a finer grain size d_{50} of 210 nm ($d_{10} = 90 \text{ nm}$, $d_{50} = 520 \text{ nm}$) but a broader particle size distribution. The size fraction above 1 μm is probably an artifact of the granulometry measurement as the peak shifted in size and location with ultrasonic treatment.

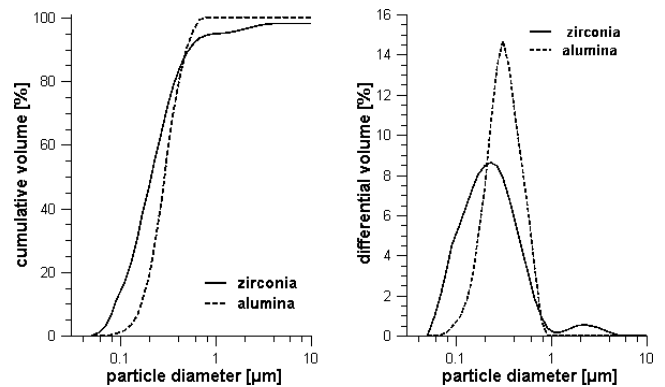


Fig. 1: Cumulative (left) and differential (right) particle size distributions of alumina APA0.5 and zirconia UEP determined with laser granulometry.

The primary crystallite size of the zirconia powder measured by means of Scherrer analysis was $30.6 \pm 1 \text{ nm}$. Thus – given that geometry is spherical – every agglomerate consists of a few hundred primary crystallites. Larger hard agglomerates are absent. The chosen powder is suitable to produce a ZTA with nanocomposite architecture without powder-related zirconia agglomerates. Processing-related agglomerates may still occur.

(2) Mechanical properties

The Vickers hardness values of the ZTA materials is shown in Fig. 2. The macrohardness HV_{10} is relatively constant over the covered sintering temperature range and has only a slight tendency to decline with rising temperature from 1980 to 1930 HV_{10} . The microhardness reacts more sensitively to changes in grain size. $HV_{0.1}$ is initially very high (~2400) and declines with rising sintering temperature. Between 1475 °C and 1500 °C a clear drop in microhardness is observed, this effect may not be caused by grain growth alone but also by a change in phase composition. Growth of zirconia grains over the critical size leads to formation of monoclinic phase, which may introduce microcracks and thus reduce hardness and stiffness. The initial rise in microhardness from 1400–1425 °C sintering temperature hints at incomplete densification at the lowest temperature. This assumption was not confirmed

by the measured density values (Fig. 3). Concerning the density values measured, it should be pointed out that no constant density can be assumed if the phase composition of zirconia changes, transformation of 50% of the tetragonal phase to monoclinic will reduce the density by 0.5 %.

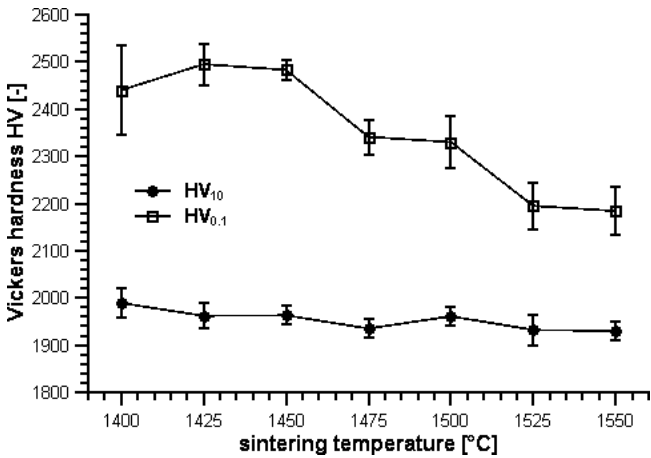


Fig. 2: Vickers hardness HV_{0.1} and HV₁₀ of ZTA vs. sintering temperature.

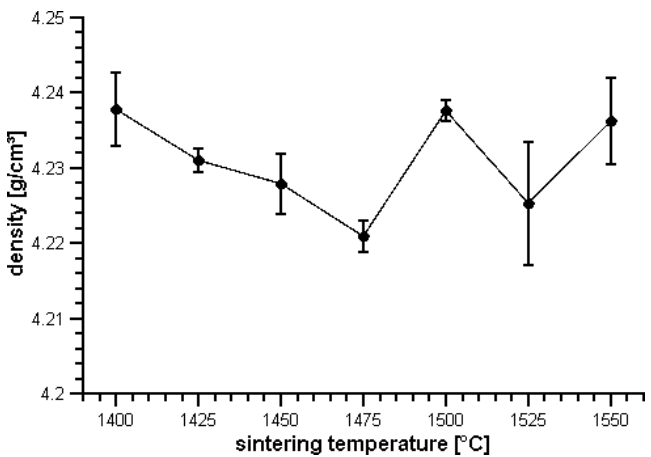


Fig. 3: Apparent density of ZTA vs. sintering temperature.

The fracture toughness measurement was performed with two independent procedures (Fig. 5). Applying the formalism of Lange to a ZTA with 10 vol% of pure tetragonal zirconia of 0.5 μm grain size, we can expect a toughness increment of 0.9 MPa·√m added to the level defined by the rule of mixture for alumina with 10 vol% untransformable zirconia. This corresponds to an absolute toughness of ~4.4 MPa·√m¹⁴. In reality not all the zirconia inclusions have the same grain size. Therefore the real toughness increase derived from transformation toughening is lower. We can expect that the size of the zirconia inclusions grows with rising sintering temperatures. Hence the larger grains – d₉₀ of the zirconia is already at the threshold value for transformation in the starting powder – will exceed the critical size while the smaller grains will successively approach the critical grain size. With increasing sintering temperatures a more complex transition between reinforcement mechanisms will take place than in an idealized case with uniform inclusion sizes.

The measured toughness level is very attractive for a nanocomposite ZTA with only 10 vol% reinforcement. At low sintering temperatures K_{ISB} is in the range

~4–4.2 MPa·√m, a value in good accord with Lange’s prediction. At high temperatures the toughness seems to level out at 5–5.25 MPa·√m, this indicates a rising contribution by microcrack toughening.

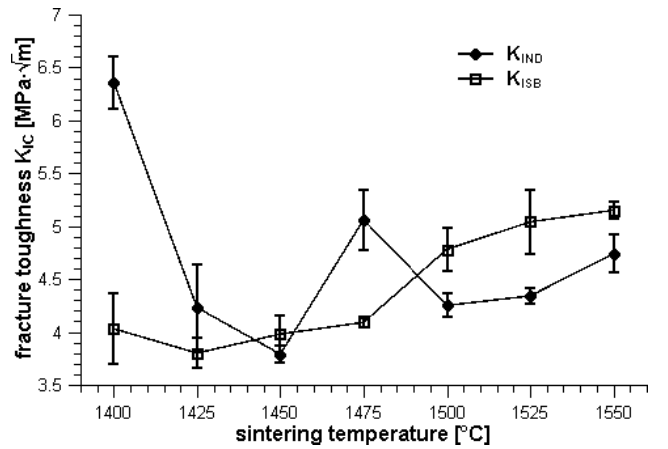


Fig. 4: Fracture toughness K_{IC} determined with the direct crack length measurement (K_{IND}) and residual strength method (K_{ISB}) of ZTA vs. sintering temperature.

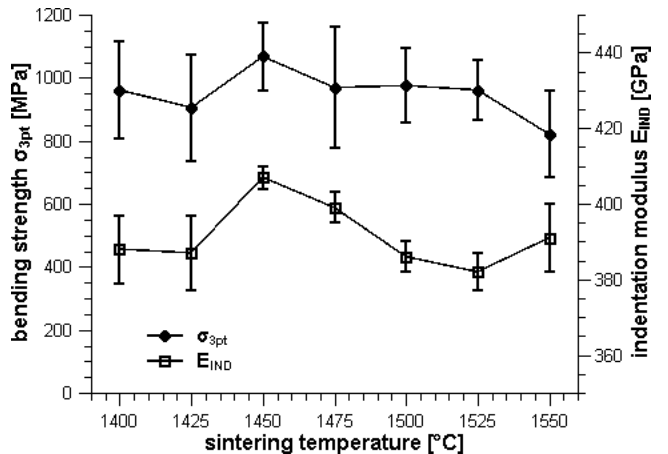


Fig. 5: Bending strength σ_{3pt} and indentation modulus E_{IND} of ZTA vs. sintering temperature.

The differences between residual strength and direct crack measurement are worth discussing in more detail. Toughness determination based on direct crack length measurements has recently suffered from harsh criticism¹⁵. However, it was more or less accepted that, even if the direct crack length measurements may be incorrect concerning the absolute toughness values, they still show the correct trend in toughness. Results show that in the present case neither trend nor absolute values are correct. From basic considerations we may deduce that the transformability of the intergranular tetragonal zirconia grains rises with increasing grain size until a threshold value of ~0.5 μm is reached, then the grains turn monoclinic during cooling from sintering temperature. These monoclinic grains provide no transformation toughening and are too small to lead to significant microcracking. The toughness contribution by microcracking rises with further increase in grain size. This simple correlation leads to toughness values rising with increasing sintering temperature – precisely this relationship was found with the

residual strength method. The slightly higher toughness at the lowest sintering temperature is in the range of standard deviations.

Direct crack length measurements in transformation toughened materials may be sensitive to surface effects like compressive stresses introduced by machining or by the indentation process itself. This may induce some toughness artifacts such as the extremely high value for ZTA sintered at 1400 °C which have no counterpart in reality.

The bending strength and indentation modulus are shown in Fig. 5. We can see a high strength level over almost the entire sintering temperature range and a strength maximum of 1067 MPa at 1450 °C. The drop in strength above 1525 °C is probably associated with the growth of the zirconia grains and the formation of monoclinic phase, which contributes to toughness but not to strength. Despite the fact that identical processing and machining conditions should lead to identical flaw sizes, no direct correlation between strength and toughness is observed.

(3) Phase analysis

The fraction of monoclinic present in polished samples sintered at different final temperature is shown in Fig. 6. As the zirconia fraction in the composites is only 10 vol%, the signal intensities are generally lower than in case of TZP. In the case of the fractured faces this inevitably leads to high standard deviations. As we can expect, the monoclinic content rises with increasing sintering temperature from 22 to 52 vol%.

Phase analysis of the fracture faces shows a similar trend. The transformability, defined as the difference in volume content of monoclinic phase in fractured face and polished surface, shows an interesting tendency. Transformability rises with rising sintering temperature up to 1450 °C, breaks down to almost zero at 1475 °C and rises again with a further temperature increase. (Note that the high standard deviations in calculation of the transformability by subtraction of the volume content in the polished and the fractured surface add up and that a high level of uncertainty exists).

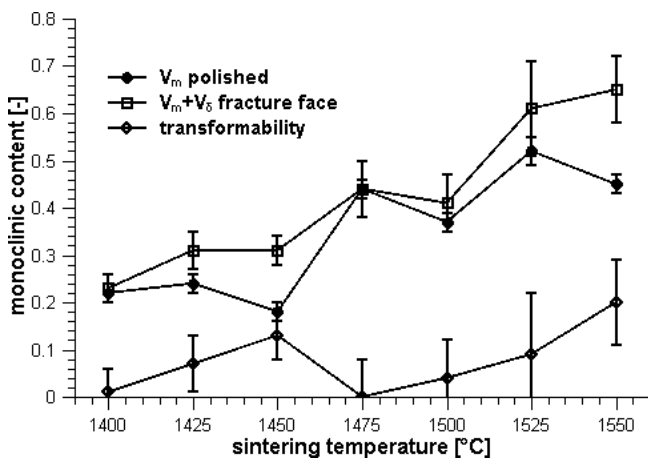


Fig. 6: Monoclinic content in polished surface and fracture face, transformability of tetragonal zirconia in ZTA vs. sintering temperature.

Experimental findings of phase analysis add another aspect to the above discussion of toughness. Evolution of residual stress has to be taken into consideration in the explanation of toughness evolution. The low-temperature (< 1475 °C)-sintered ZTA materials have a monoclinic content of ~20 %, which is close to the stress neutral state⁷. Above this temperature, the monoclinic content rises and zirconia is under compressive stress and presumably becomes less transformable. The surrounding alumina matrix is then under tensile stress, which favors the formation of microcracks. Microcracking locally reduces the Young's modulus of the matrix, which facilitates further phase transformation. In the present case on a macroscopic level no evidence of decreasing Young's modulus was detected.

In addition to the monoclinic phase, another structure is formed after fracture in some of the samples (Fig. 7). Two reflexes at 29.1 and 29.5° 2 θ appear. This effect was recently also found in TZP of high toughness and transformability¹⁶. The reflexes hint at a structural motif of rhombohedral symmetry with a δ -phase structure (like $Y_4Zr_3O_{12}$) formed during phase transformation. The fact that the reflexes appear in yttria-free ZTA proves that this is not yttrium zirconate but a zirconia structure.

The correlation between phase composition, strength and toughness is rather complex. At peak strength we observe low toughness, high transformability and the lowest monoclinic content in all samples. We may assume that monoclinic phase in the as-fired sample is detrimental to strength and that the strength is mainly improved by transformation toughening. At a sintering temperature of 1550 °C an equally high transformability is measured but at a much higher content of monoclinic phase, which provides additional toughness but is believed to diminish strength. A glance at the position of the tetragonal (101) reflex shows different peak shifts on the 2 θ -scale at different sintering temperatures. This indicates that residual stresses may also influence the toughness level and lead to falsification of the direct crack length measurements¹⁷.

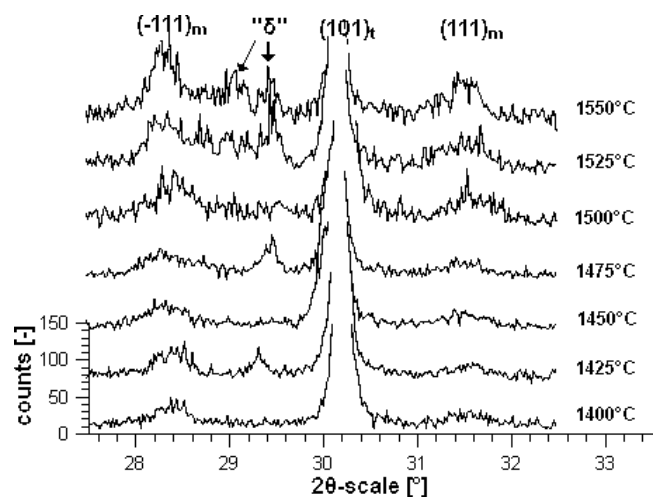


Fig. 7: XRD investigation of the fracture face of ZTA in the 27–33° 2 θ -range.

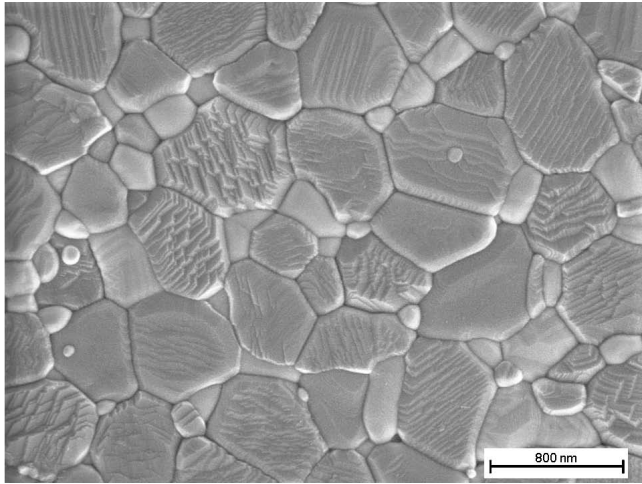


Fig. 8: SEM image of ZTA sintered at 1400 °C (polished and thermally etched surface (1400 °C/30 min/air))

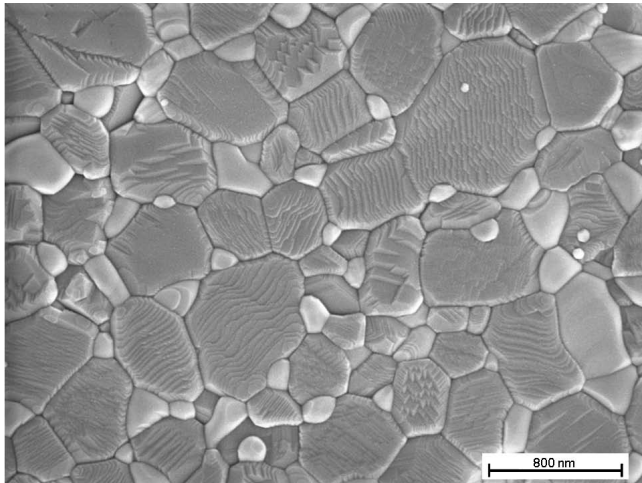


Fig. 9: SEM image of ZTA sintered at 1450 °C (polished and thermally etched surface (1400 °C/30 min/air)).

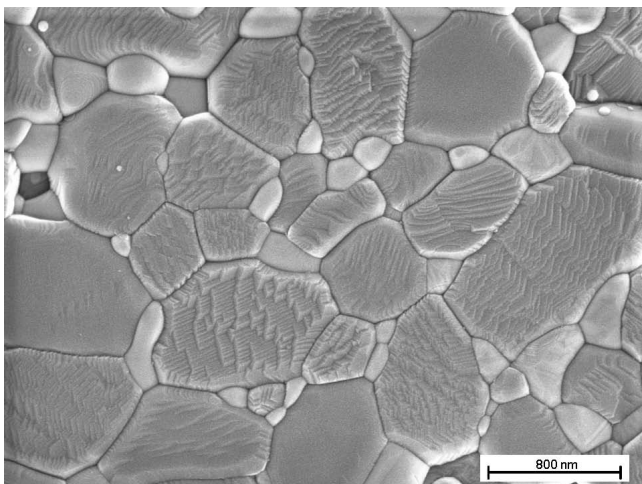


Fig. 10: SEM image of ZTA sintered at 1500 °C (polished and thermally etched surface (1400 °C/30 min/air)).

(4) *Microstructure*

The microstructural analysis (Figs. 8–11) performed with SEM can help explain the questions emerging after mechanical characterization and phase analysis. Zirconia grains are predominantly located at grain boundaries;

intragranular zirconia grains are very rare. The quality of dispersion is very good as all the zirconia grains in the samples sintered at 1400 °C are small and isolated. A moderate but clear tendency to coarsening is visible with rising sintering temperatures. Fig. 12 shows the grain sizes of alumina and zirconia vs. sintering temperatures. The average alumina grain sizes rise from ~700 nm to 1000 nm while zirconia grains grow from initially 300 nm to 450 nm. The rise in grain size is not linear, the initial grain size can be maintained until coarsening is observed between 1475–1500 °C. While the zirconia grains continue to grow slightly at higher temperatures the size of the alumina grains stays at the level reached at 1500 °C. At least the larger zirconia grains do exceed the size limit for spontaneous transformation, which partly explains the higher monoclinic content at higher sintering temperatures. Another fact to be considered is the increase of crystallinity at higher sintering temperatures⁵. What is also obvious is that with increasing heat treatment temperature > 1500 °C zirconia grains tend to leave the four junctions. Very often zirconia grains are located between two alumina grains. This mechanism was described by Lange⁴.

A final discussion of the mechanical properties of the ZTA material depending on changes in sintering conditions has to take into account all observations of the mechanical properties as such as well as observations made concerning phase composition and microstructure.

A strength level of >1000 MPa at a toughness of 4 MPa·√m according to Griffith's law for brittle materials hints at a high degree of microstructural perfection with flaw sizes in the range between 3–4 μm. With rising toughness (above sintering temperatures of 1450 °C) no further strength increase is found. Above this temperature the phase composition leaves the stress-neutral state (~20 vol% monoclinic) and a rising proportion of monoclinic phase is detected. This change of phase composition, which is mainly derived from grain growth, leads to increasing compressive stress in the zirconia and tensile stress in the alumina matrix. If the structure remained intact, the rising compressive stress on the zirconia would inhibit transformation and lower the toughness, tensile stress in the alumina matrix would favor crack propagation and loss of strength, this is, however, not the case. Instead, above a sintering temperature of 1450 °C, we observe a slight decrease of the indentation modulus, which hints at the formation of microcracks. Microcracking and proceeding transformation seem to be a self-reinforcing mechanism as the microcracked matrix facilitates further transformation, which then triggers further microcracking. Thus with further rising sintering temperatures we observe a rising level of monoclinic as well as a rising transformability. Only in this situation does it become possible to exploit both toughening effects. Microcracking does not, however, substantially contribute to strength. An increasing microcracking process will finally result in flaw sizes exceeding the sizes of flaws typically derived from processing. In this situation strength will tend to decline but rising toughness can to a certain extent counteract this trend. It is thus not desirable to

trigger too extensive microcracking as this would result in extreme toughness but only moderate strength. From the view point of ceramic materials design it seems that controlling the microstructural features —well-dispersed zirconia grains of defined size in a fine-grained relatively rigid alumina matrix— is the key to obtain ZTA with both high strength and toughness.

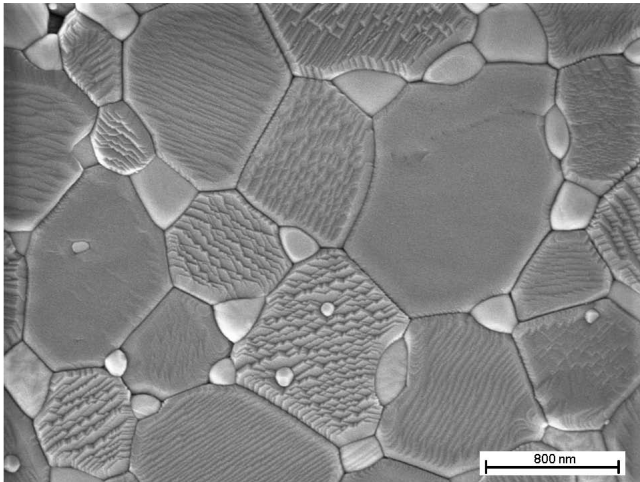


Fig. 11: SEM image of ZTA sintered at 1550 °C (polished and thermally etched surface (1400 °C/30 min/air)).

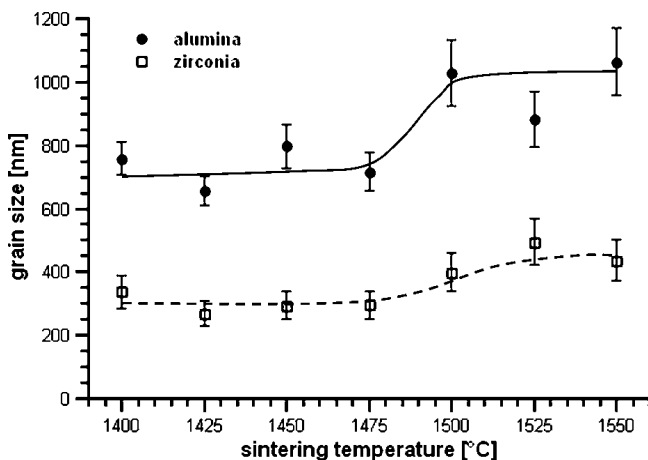


Fig. 12: Grain sizes of alumina and zirconia estimated from SEM images with the line intercept method.

IV. Summary and Conclusion

Zirconia-toughened alumina with nanocomposite structure was manufactured by means of hot pressing. The distribution of the zirconia dispersion is close to perfection even when a mixing and milling approach is used. Mechanical properties – strength, hardness and toughness – are very attractive for a ZTA with only 10 vol% reinforcement and come close to the values required for biomedical grade ZTA. Rising sintering temperatures lead to a coarsening of the microstructure, which results in a change in mechanical properties. The increasing size of the zirconia inclusions provides a rising level of toughness. While the zirconia is initially ~80 % tetragonal, monoclinic content rises with sintering temperature. XRD data prove that the toughness increase below 1475 °C is purely transformation-related. After an intermediate breakdown in trans-

formability, the higher toughness at high sintering temperatures is determined by a rising contribution of both microcracking and transformation toughening. The strength of the composites appears to be predominantly defined by transformation toughening.

The interpretation of the cooperative effects of reinforcement mechanisms is quite complex. A high level of monoclinic content promotes microcracking and is detrimental to strength.

Without changing the basic composition, further improvements of the mechanical properties may be possible by using a zirconia starting powder with more uniform grain size. In future the research will focus on transferring the material-science-related results of this study to performing manufacturing technologies like axial pressing or ceramic injection molding and preferentially pressureless sintering to gain access to technically relevant application fields like biomedical implants and mechanical engineering components.

References

- Hannink, R., Kelly, P., Muddle, B.: Transformation toughening in zirconia-containing ceramics, *J. Am. Ceram. Soc.*, **83**, [3], 461–87, (2000).
- Claussen, N.: Fracture toughness of Al_2O_3 with an unstabilized ZrO_2 dispersed phase, *J. Am. Ceram. Soc.*, **59**, [1–2], 49–51, (1976).
- Wang, X., Tian, J., Yu, X., Shan, Y., Liu, Z., Yin, Y.: Effect of microstructure on the fracture behavior of micro-nano ZTA composite, *Mat. Chem. Phys.*, **112**, 213–217, (2008).
- Lange, F.F., Hirlinger, M.: Hindrance of grain growth in Al_2O_3 by ZrO_2 inclusions, *J. Am. Ceram. Soc.*, **67**, [3], 164–168, (1982).
- Heuer, A.H., Claussen, N., Kriven W.M., Rühle, M.: Stability of tetragonal ZrO_2 particles in ceramic matrices, *J. Am. Ceram. Soc.*, **65**, [12], 642–650, (1982).
- Lange, F.F.: Transformation toughening, part 4: Fabrication, fracture toughness and strength of Al_2O_3 - ZrO_2 composites, *J. Mat. Sci.*, **17**, 247–254, (1982).
- Gregori, G., Burger, W., Sergio, V.: Piezo-spectroscopic analysis of the residual stresses in zirconia-toughened alumina ceramics: the influence of the Tetragonal-to-monoclinic transformation, *Mater. Sci. Eng.*, **A271**, 401–406, (1999).
- DeAza, A., Chevalier, J., Fantozzi, G., Schehl, M., Torrecillas, R.: Slow-Crack-growth behavior of zirconia-toughened alumina ceramics processed by different methods, *J. Am. Ceram. Soc.*, **86**, [1], 115–20, (2003).
- Patterson, A.L.: The scherrer formula for x-ray particle size determination, *Phys. Rev.*, **56**, 978–982, (1939).
- Anstis, G.R., Chantikul, P., Lawn, B.R., Marshall, D.B.A.: A critical evaluation of indentation techniques for measuring fracture toughness. I. Direct crack measurements, *J. Am. Ceram. Soc.*, **64**, 533–538, (1981).
- Chantikul, P., Anstis, G.R., Lawn, B.R., Marshall, D.B.A.: A critical evaluation of indentation techniques for measuring fracture Toughness. II. Strength method, *J. Am. Ceram. Soc.*, **64**, 539–543, (1981).
- Toraya, H., Yoshimura, M., Somiya, S.: Calibration curve for quantitative analysis of the monoclinic-tetragonal ZrO_2 system by x-ray diffraction, *J. Am. Ceram. Soc.*, **67**, [6], C119–121, (1984).
- Mendelson, M.I.: Average grain size in polycrystalline ceramics, *J. Am. Ceram. Soc.*, **52**, 443, (1969).

- ¹⁴ Lange, F.F.: Transformation toughening, part 3: Experimental observations in the ZrO_2 - Y_2O_3 System, *J. Mat. Sci.*, **17**, 240–246, (1982).
- ¹⁵ Quinn G.D., Bradt R.C.: On the vickers indentation fracture toughness test, *J. Am. Ceram. Soc.*, **90**, [3], 673–680, (2007).
- ¹⁶ Kern, F: Properties of 2.5Y-TZP manufactured from alumina-doped yttria-coated pyrogenic zirconia nanopowder, *J. Ceram. Sci. Tech.*, **2**, [2], 89–96, (2011).
- ¹⁷ Kern, F: Microstructure and mechanical properties of hot-pressed alumina 5 vol% zirconia nanocomposites, *J. Ceram. Sci. Tech.*, **2**, [1], 69–74, (2011).

